

1 A study of Cobalt (II) complexes involved in marine biogeochemical
2 processes: Co(II)-1,10-Phenanthroline and Co(II)-1,10-Phenanthroline-L-
3 α -Phosphatidylcholine

4

5 Anđela Bačinić^a, Sanja Frka^a, Marina Mlakar^{a,1*}

6 ^aRuđer Bošković Institute, Division for Marine and Environmental Research, Bijenička
7 street 54, P.O. Box 180, 10000 Zagreb, Croatia

8 ¹ ISE member

9 *corresponding author – mlakar@irb.hr

10

11 Abstract

12 The cell membrane is structured so that the surface layer is composed of lipid
13 molecules with selective permeability for micronutrients and organic ligands. Binding
14 of Co (II) to natural lipid phosphatidylcholine (PC) has been studied to identify a
15 possible mechanism of Co (II) entry through the cell membrane of the biota in detail,
16 by voltammetry followed by checking the system at the air-water boundary, by
17 Langmuir method. Binding of cobalt (II) ions to the PC molecules was enabled by the
18 Co(II)-1,10-Phenanthroline (Phen) complex formation as an intermediate. Co(II)-
19 Phen-PC complex reduction was recorded in the pH range from 5 to 9.5. The
20 reduction was identified as a two-electron irreversible reaction at about -1.5 V, with
21 the reactant adsorption followed dissociation (EC mechanism). The Co(II)-Phen-PC
22 complex electrode surface concentration (Γ) was calculated to be $(1.45 \pm 0.12) \times 10^{-10}$
23 mol
24 cm⁻². Conditional stability constants $K_{\text{Co(II)Phen}_2\text{PC}} = 23.02 \pm 0.26$ and $\log K_{\text{Co(II)Phen}_2\text{PC}_2}$

25 = 29.31 ± 0.17 ($I_c = 0.55$) were calculated by CLE/ACSV method. Pressure-area (π -
26 A) isotherms obtained at water-air interface by Langmuir monolayer technique
27 indicated penetration of Co(II)-Phen into the PC monolayer, supporting
28 electrochemical results. The equilibrium constants of the Co (II)-PC system (1:1) at
29 the air-water interface was calculated to be $K_1 = 2.4 \times 10^{-2} \text{ m}^3 \text{ mol}^{-1}$, while for Co(II)-
30 Phen-PC $K_2 = 4.86 \times 10^{10} \text{ m}^2 \text{ mol}^{-1}$.

31

32 **Keywords:** Cobalt (II), 1,10-Phenanthroline, Phosphatidylcholine, Voltammetry,
33 Langmuir trough

34

35 1. Introduction

36 Cobalt is an essential trace element important for the functioning of all organisms,
37 including biota in the marine environment [1]. Micronutrient ions play a variety of
38 important roles in biota and complexation by organic ligands drives their chemical
39 speciation. Namely, cobalt is an important co-factor in vitamin B12-dependent
40 enzymes [2]. Studies on cobalt ions in the marine environment, which define their
41 behavior associated with interactions with cell membranes, have been poorly
42 described in the literature. Identification of the formation mechanism of natural
43 organic ligands is fundamental for determining the micronutrients speciation and
44 determining their bioavailability [3,4]. Cobalt ion express the nutrient profile and
45 shows high reactivity in seawater related to the functioning of the biota. The
46 complexation of cobalt ions in the marine environment is predominant by organic
47 ligands and it suggests the biological control through the production of organic cobalt
48 complexes [5,6]. Studies have shown that cyanobacteria produce cobalt complexing

49 ligands [7]. For some strains such as *Synechococcus*, cobalt is necessary for their
50 growth and development, however, some can substitute zinc for cobalt in trace metal
51 limited areas, such as *Prochlorococcus*. The best-known ligands that bind cobalt are
52 vitamin B12 and coenzyme B12 [8,9]. The stability constants for these ligands are
53 extremely high ($\log K > 17$). 1,10-Phenanthroline ($C_{12}H_8N_2$, Phen) is a heteroaromatic
54 compound whose nitrogen atoms are arranged perfectly to bond various cations [10],
55 is often used as humic/fulvic acid model ligand in natural waters [11], as well as
56 vitamin B12.

57 Two general features of phospholipid bilayers are critical to membrane function [12].
58 First, the structure of phospholipids is responsible for the basic function of
59 membranes as barriers between two aqueous compartments. Hydrophobic fatty acid
60 chains occupy the interior of the phospholipid bilayer making the membrane
61 impermeable to water-soluble molecules, including metal ions and most biological
62 molecules. Second, bilayers of naturally occurring phospholipids are viscous liquids
63 [13]. The fatty acids of most natural phospholipids have one or more double bonds
64 that introduce kinks into the hydrocarbon chains and make them difficult to pack
65 together. Therefore, the long hydrocarbon chains of the fatty acids move freely inside
66 the membrane, making it soft and flexible [14]. In model solutions metal ions are most
67 often coordinated with carboxylate and NH groups [15,16]. Phospholipid monolayers
68 absorbed at model hydrophobic interfaces, such as the mercury electrode surface
69 and air-water interface, actually represent a biological membrane model system
70 [17,18]. Some studies reported interactions of metal ions, drugs, toxins, and
71 biologically important species with model phospholipid monolayers [19-22].
72 Additionally, liposomes are frequently used as unilamellar or multilamellar spherical
73 structures in studies of biological model membranes [23]. Adsorption of organic

74 molecules to the phospholipid membrane causes a change in membrane surface
75 potential and/or modifies its dipole potential. Interactions of micronutrient ions with
76 cells through membranes in the marine environment are of particular interest as they
77 are critical for the maintenance of cellular function [24].

78 The aim of this study was to investigate the interaction/binding mechanism of Co(II)
79 with phospholipids, as a vital component of hydrophobic cell membranes, following
80 the formation of their complexes through an intermediate, Co(II)-Phen complex.

81

82 **2. Experimental**

83 **2.1. Chemicals and solutions**

84 L- α -phosphatidylcholine (PC; *Sigma-Aldrich*, egg yolk, type XVI-E, $\geq 99\%$ (TLC)) as
85 lyophilized powder was used in this study. The components of the PC commonly
86 present in natural seawater, contain approximately 33% 16:0 (palmitic acid), 13%
87 18:0 (stearic acid), 31% 18:1 (oleic acid) and 15% 18:2 (linoleic acid) (other fatty
88 acids in a smaller amounts), resulting in an average molecular weight of
89 approximately 768 g mol^{-1} . The original stock solution was kept at 253.15 K. PC
90 solution for electrochemical measurements was prepared by dissolution in methanol
91 ($1 \times 10^{-2} \text{ mol dm}^{-3}$) (p.a. *Kemika d.d.*, Zagreb, Croatia). Methanol stock solution of
92 PC was added in to the NaCl solution ($1 \times 10^{-5} \text{ mol dm}^{-3}$) and by the accumulation
93 monolayer was formed by the accumulation at $E_{acc} = 0.0 \text{ V}$ vs Ag/AgCl (Fig S1A,B).
94 For the monolayer experiments by Langmuir method the PC stock chemical (0.5 mg
95 cm^{-3}) was dissolved in hexane of HPLC grade (Merck) and monolayer was formed at
96 the NaCl surface by the syringe applying. A stock solution ($1 \times 10^{-3} \text{ mol dm}^{-3}$) of
97 1,10-Phenanthroline ($\text{C}_{12}\text{H}_8\text{N}_2$, Phen) (p.a., Merck), was dissolved in ultraclean water.

98 NaCl (Suprapur[®], Merck, Germany) as electrolyte solution ($I_c = 0.55 \text{ mol dm}^{-3}$) was
99 prepared by dissolution in Milli-Q water. A standard solution of Co(II) nitrate ($1.69 \times$
100 $10^{-2} \text{ mol dm}^{-3}$) (Fluka Chemie GmbH, Buchs, Switzerland), as the source of cobalt (II)
101 in all experiments, was used.

102

103 **2.2. Electrochemical measurements**

104 Voltammetry studies were performed by μ -AUTOLAB multimode potentiostat (ECO
105 Chemie, Utrecht, the Netherlands) using Metrohm 663 VA stand (Metrohm, Herisau,
106 Switzerland). The instrument was computer-controlled using GPES 4.9 control
107 software, while a static mercury drop electrode (SMDE, size 2, i.e. 0.40 mm^2) was
108 working electrode, a glassy carbon stick counter electrode and Ag/AgCl (sat. NaCl)
109 ($+0.197 \text{ V vs. SHE}$) reference one. Experiments were done in quartz cell at $25 \pm 1 \text{ }^\circ\text{C}$
110 in NaCl of $I_c = 0.55 \text{ mol dm}^{-3}$ ($I_c =$ ionic strength). Voltammetric methods used were
111 alternating current (AC), square-wave (SWV) and cyclic technique (CV). Solutions
112 were deaerated by bubbling with extra pure nitrogen for about 20 min with stirring
113 (3000 rpm) before measurements, while during measurements, nitrogen circulated
114 above the solution. pH was measured by glass-Ag/AgCl electrode linked to ATI Orion
115 PerpHecTMeter, model 320 (Cambridge, USA). All relevant measurements were
116 repeated for three times, at least.

117

118 **2.3. Surface pressure measurements**

119 Surface pressure-area (π -A) measurements were performed in a Fromherz-type
120 round Teflon trough (Mayer-Feinttechnik, Germany), equipped with two movable
121 barriers. Surface pressure was performed at $21 \text{ }^\circ\text{C}$ with a precision $\pm 0.1 \text{ mN m}^{-1}$

122 using a Wilhelmy plate (Whatman filter paper, No. 1) as pressure sensor. On the
123 initial surface area ($A_{\max} = 160 \text{ cm}^2$), the PC monolayer was formed by carefully
124 applying aliquots ($V = 0.02 \text{ cm}^3$) of the PC solution in hexane (0.5 mg cm^{-3}) onto the
125 subphase using a microsyringe (Hamilton–Bonaduz, Switzerland). The supporting
126 monolayer was left for 3 h to allow the incorporation of the subsurface components
127 within the monolayer. The monolayer was further compressed at a rate of 60 cm^2
128 min^{-1} , and changes in surface pressure due to changes in molecular packing of the
129 formed monolayer were followed while π - A isotherms were recorded. The monolayer
130 was compressed up to the compression limit of 40 mN m^{-1} , prior to collapse.
131 Consistency and the reproducibility of results were ensured by repeating each
132 measurement at least five times. The limiting area per molecule, A_{lim} , was determined
133 conventionally by extrapolating the linear part of the obtained π - A isotherm to $\pi = 0$
134 mN m^{-1} , which corresponds to the cross-sectional area of the maximally ordered
135 molecule for a given monolayer. The trough and barriers were cleaned after each run
136 with hexane and Milli-Q water.

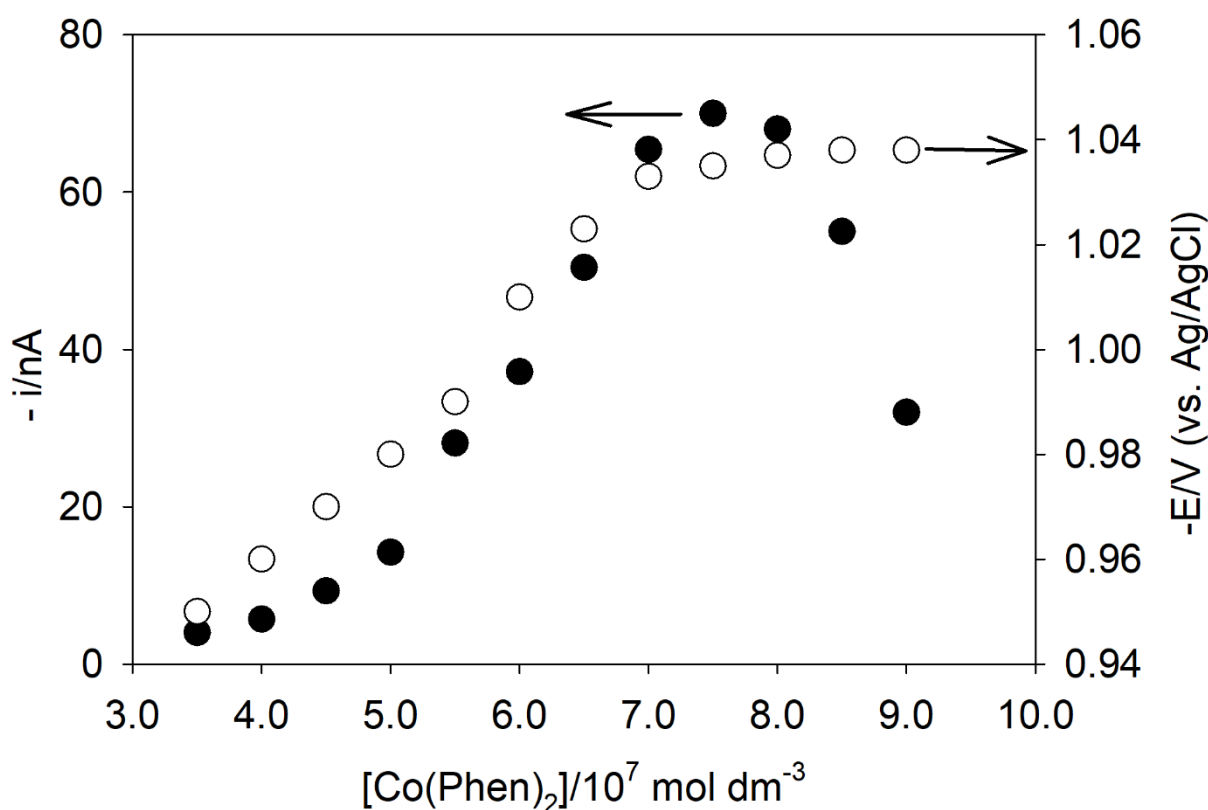
137

138 **3. Results and Discussion**

139 **3.1. Voltammetric characterization of Co (II)-1,10-Phen and Co (II)-1,10-Phen-PC** 140 **complex**

141 Lipid membranes attached to the mercury drop electrode surface are highly
142 promising biomimetic membranes for the elucidation of structure-function
143 relationships micronutrients in the environment [25]. Investigations of the potential
144 interactions of Co(II) with PC were carried out using square wave (SW), alternating
145 current (AC) out of phase mode (tensametry, phase angle 90°) and cyclic
146 voltammetry (CV). We anticipated a simple binding mechanism between PC with

147 Co(II) via Co(II)-PC complexes formation, however, our results advocated rather
148 more complex reaction pathway. The introduction of 1,10-Phenanthroline (Phen) as
149 an intermediate ligand led to the formation of Co(II) mixed ligand complex with PC.
150 According to our previous investigations, Co(II) complexes bind mainly to nitrogen-
151 containing organic ligands [16]. Its entropic advantage indicates fast formation of very
152 stable complexes with metal ions, especially with transition metals. The Phen ligand
153 behaves like a weak base in aqueous solution with $pK_a \sim 4.9$. Alternating current
154 voltammograms (ACV) indicate moderate adsorption of Phen at the mercury drop
155 electrode surface due to aromatic structure in the potential range from -0.1 to -1.6 V.
156 By adding Co (II) to the Phen solution complex SW reduction peak appears at about -
157 1.0 V (pH = 8.2). pH dependence of the Co(II)-Phen complex reduction current
158 showed an increase in the pH range from 3.5 to 5.0, while it remained constant at
159 higher pH values (up to pH 9). By titration of Phen ($1 \times 10^{-6} \text{ mol dm}^{-3}$) with Co(II) in
160 the range from 1×10^{-7} to $1 \times 10^{-6} \text{ mol dm}^{-3}$, the reduction current of the complex (E_p
161 $\approx -1.0 \text{ V}$) increased until $c_{Co} = 8 \times 10^{-7} \text{ mol dm}^{-3}$ (Fig.1). With higher Co(II)
162 concentrations reduction current decreased due to saturation of the mercury drop
163 surface with Co(II)-Phen molecules, due to a reduction process inhibition. The
164 reduction potential of Co(II)-Phen changed slightly towards negative values (Fig 1).

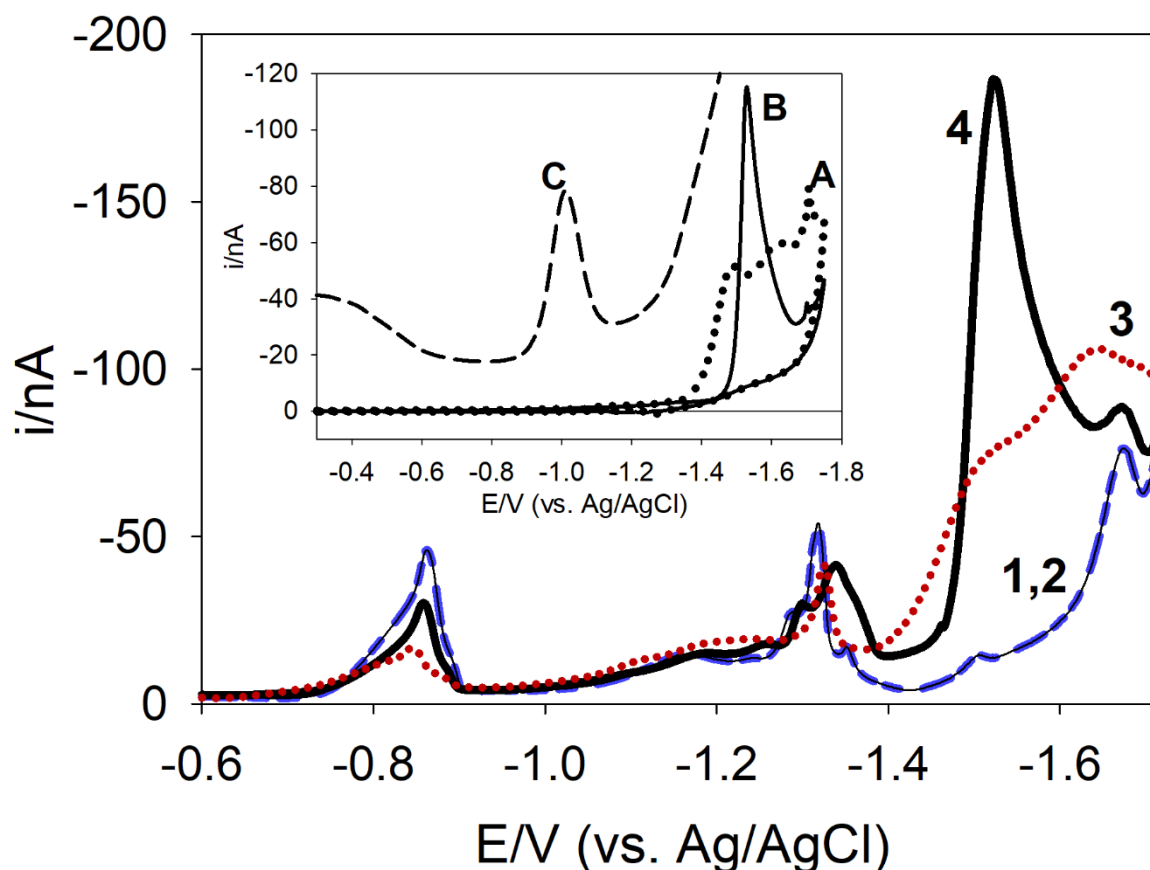


165
 166 Fig 1. Dependence of (●) peak current and (○) peak potential of the Co(Phen)₂
 167 complex on c_{Co} in range from 1×10^{-7} to 1×10^{-6} mol dm⁻³; $c_{\text{Phen}} = 1 \times 10^{-6}$ mol dm⁻³,
 168 $E_{\text{acc}} = 0$ V, $t_{\text{acc}} = 180$ s, $f = 50$ s⁻¹, $a = 25$ mV.

169 Furthermore, interaction of Co(II) with PC was investigated. The ACV point to PC
 170 adsorption in the potential range from about -0.1 V and desorption at potential
 171 > -1.65 V (Fig. S1A). The capacitive peak registered at about -1.1 V represents the
 172 reorientation process of PC molecules as the consequence of charging current,
 173 revealing structural/electrostatic changes in the adsorbed lipid layer from flat to
 174 perpendicular position [16, 24-26]. No interaction of PC with Co (II) ions was
 175 recorded on SW voltammograms (Fig 2, curve 2). The sequence of the ligands
 176 (Phen, PC) addition to the solution revealed to be very important. Namely, the
 177 hydrophobic ligand – PC adsorbs at the mercury drop surface by the accumulation,
 178 and added Phen adhere to the PC layer and only slightly affects the surface

179 organization of its monolayer (Fig. 2, curve 3). With the addition of Co(II) to the
180 solution of both ligands, neutral hydrophilic Co(II)-Phen complex forms in the solution
181 and by the accumulation at the electrode surface creates hydrophobic mixed ligand
182 complex. Namely, PC molecules replace the remaining water molecules from the
183 Co(II) ion coordination sphere. As described in the literature, the ion channels open
184 in response to the initiating stimulus [27]. In ligand-gated channels, ligand-binding
185 domains are attached to the pore in the adsorption layer at the electrode surface. In
186 neutral ligand channels attached to the electrode surface, the parts that bind the
187 hydrophilic complex are in the pores of the adsorption layer. Therefore, the Co(II)-
188 Phen complex as intermediate assisted Co(II) mixed ligand complex formation with
189 lipid. Co(II)-Phen-PC complex in the adsorption layer allows the electron path from
190 the electrode to Co(II) ion through the ligand gated channel. A sharp reduction signal
191 at about -1.5 V was registered as Co(II) was added to the solution of both ligands
192 present (Fig. 2, curve 4) and it is assigned to two-electron reduction of Co(II)-Phen-
193 PC complex. After reduction process mixed ligand complex dissociate (Fig. 2, CV
194 inset), only the PC layer remains on the electrode surface, as evident when two
195 subsequent scans were performed at the same Hg drop.

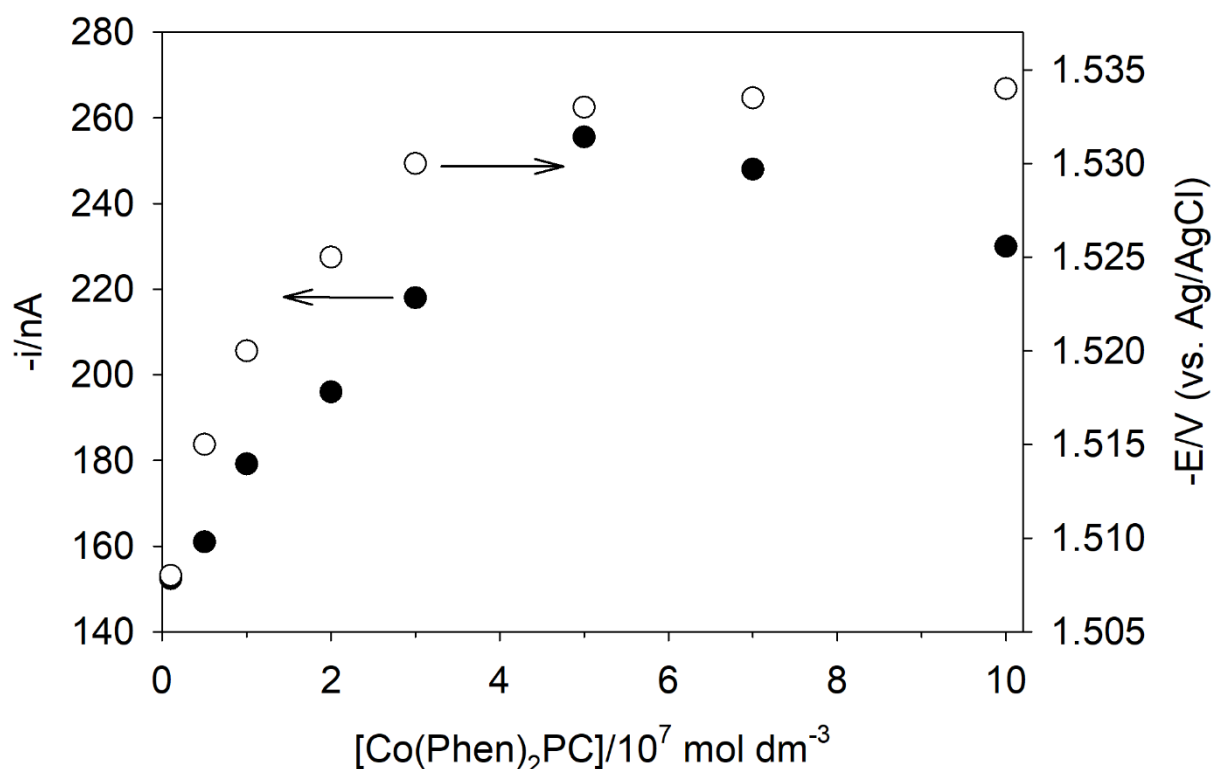
196 Accumulation time as well as accumulation potential variation influenced on the
197 amount of adsorbed mixed ligand complex at the electrode. The reduction peak of
198 Co(II)-Phen-PC complex increased with the variation of the accumulation potential
199 between -0.3 and -1.3 V. With $E_{acc} = -1.3$ V for 3 minutes or more, it was calculated
200 that by SWV measurable Co (II) concentrations would be down to 10^{-10} mol dm⁻³.



201
 202 Fig 2. SW voltammograms of $c_{PC} = 1 \times 10^{-5} \text{ mol dm}^{-3}$, $c_{Phen} = 10^{-6} \text{ mol dm}^{-3}$, $c_{Co} = 5 \times$
 203 $10^{-7} \text{ mol dm}^{-3}$; 1) PC, 2) PC+Co, 3) Phen+PC, 4) Phen+PC+Co; $E_{acc} = -0.3 \text{ V}$, $t_{acc} = 60$
 204 s , $E_{step} = 2 \text{ mV}$, $a = 25 \text{ mV}$, $f = 25 \text{ s}^{-1}$; inset: CV of Co(II)-Phen-PC, 2 scans at the
 205 same mercury drop; **A** first plot, **B** second plot; **C** Co(II)-Phen linear scan
 206 voltammogram; $c_{Phen} = 10^{-6} \text{ mol dm}^{-3}$, $c_{Co} = 1 \times 10^{-6} \text{ mol dm}^{-3}$; $E_{acc} = -0.3 \text{ V}$, $t_{acc} = 180$
 207 s , $v = 50 \text{ mV s}^{-1}$; $0.55 \text{ mol dm}^{-3} \text{ NaCl}$, $\text{pH} = 8.2$.

208
 209 The Co(II)-Phen-PC complex was registered in the pH range from 5 to 9, largely
 210 corresponding to the pH range in which Co(II)-Phen is present in solution. In the pH
 211 range from 5 to 8 the reduction current of Co(II)-Phen-PC complex increased, while
 212 at higher pH values current decreased due to the formation of Co (II) hydroxides.
 213 Simultaneously, the Co(II)-Phen-PC the reduction potential shifts to more negative

214 values due to the thicker layer of adsorbed complex molecules. Co(II)-Phen-PC
 215 complex reduction peak current increased linearly in the Co(II) concentration range 1
 216 $\times 10^{-9}$ mol dm⁻³ - 5×10^{-7} mol dm⁻³ with the slope 20.91 ± 0.21 nA/ μ M (Fig. 3; Fig.
 217 S2). With further additions of Co(II) to the solution, the reduction current decreased
 218 due to the redox process inhibition.

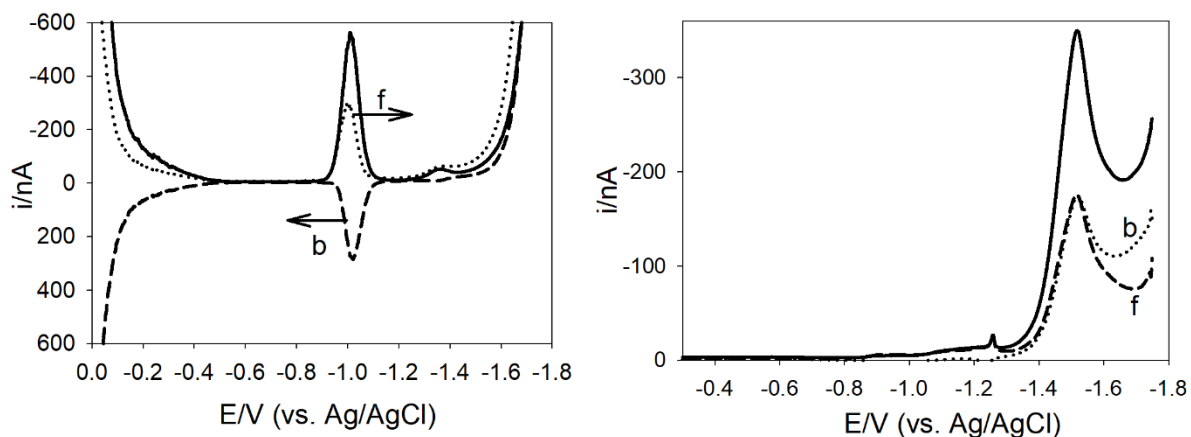


219
 220 Fig. 3. Dependence of (●) peak current and (○) peak potential of the Co-Phen-PC
 221 complex on c_{Co} in range from 1×10^{-9} to 1×10^{-6} mol dm⁻³. $c_{\text{Phen}} = 1 \times 10^{-6}$ mol dm⁻³,
 222 $c_{\text{PC}} = 1 \times 10^{-5}$ mol dm⁻³; $E_{\text{acc}} = -0.3$ V, $t_{\text{acc}} = 180$, $f = 50$ s⁻¹, $a = 25$ mV.

223
 224 **3.1.1. Estimation of the electrochemical redox process mechanisms and**
 225 **calculated conditional stability constants**

226 By SWV and CV was examined reduction process mechanisms and electrochemical
 227 characteristics of described Co (II) complexes. Their reduction peak currents and

228 potential dependencies on SW frequency, SW amplitude and CV scan rate, were
 229 measured with $c_{\text{Phen}} = 1 \times 10^{-6} \text{ mol dm}^{-3}$, $c_{\text{Co}} = 1 \times 10^{-6} \text{ mol dm}^{-3}$ pH = 8.2 for Co (II)-
 230 Phen complex. Mixed ligand complex measurements were done with $c_{\text{PC}} = 1 \times 10^{-5}$
 231 mol dm^{-3} , $c_{\text{Phen}} = 10^{-6} \text{ mol dm}^{-3}$, $c_{\text{Co}} = 5 \times 10^{-7} \text{ mol dm}^{-3}$ at $E_{\text{acc}} = -0.3 \text{ V}$ with $t_{\text{acc}} = 180$
 232 s. As SWV technique discriminates faraday and capacitive currents, and provides an
 233 insight into both half-electrode reactions, it is particularly suitable for studying the
 234 mechanisms of electrode processes [28]. The SWV response separation into forward
 235 current measured before the “down” pulse and backward, and reverse current
 236 measured at the “down” pulse of staircase, showed their reduction characteristics.
 237 SW forward-backward (f-b) showed that Co-Phen reduction process is reversible
 238 (Fig. 4 A), while of Co(II)-Phen-PC mixed ligand complex completely irreversible (Fig.
 239 4.B).



240
 241 Fig 4. backward-forward SW voltammograms of **A)** Co(II)-Phen; **B)** Co(II)-Phen-PC
 242 complexes; $c_{\text{PC}} = 1 \times 10^{-5} \text{ mol dm}^{-3}$, $c_{\text{Phen}} = 1 \times 10^{-6} \text{ mol dm}^{-3}$, $c_{\text{Co}} = 10^{-6} \text{ mol}$
 243 dm^{-3} .

244 Amplitude dependence (in the range from 5 to 50 mV) on the reduction current of the
 245 Co(II)-Phen complex increased linearly with a slope of $24.18 \pm 0.11 \text{ nAV}^{-1}$, while with
 246 A >50 mV reduction peak split in two what is characteristic for reversible reduction

247 processes from adsorbed state [29]. Reversible reduction with reactant reduction
248 Co(II)-Phen reduction current linear dependence on the scan rate (CV) in the range
249 from 1 to 100 mV/s with the slope of $1.65 \pm 0.02 \text{ nAV}^{-1}$, and shift of the reduction
250 potential towards negative values, is characteristic for reversible reduction processes
251 with the reactant adsorption [16].

252 Impact of the SW frequency and amplitude on the net reduction current (i_p) and
253 potential (E_p) on Co(II)-Phen-PC complex reduction was investigated as well. Co(II)-
254 Phen-PC complex reduction current ($E_p \sim -1.5 \text{ V}$, $t_{acc} = 60 \text{ s}$) depends linearly on f in
255 the range $8 - 300 \text{ s}^{-1}$, with the slope $21.25 \pm 0.12 \text{ nA}$, while reduction peak potential
256 dependence was linear with $\log f$ (slope $20.07 \pm 0.08 \text{ mV/d.u.}$) implying the
257 irreversible reactant reduction from adsorbed state [30]. Co(II)-Phen-PC complex
258 reduction peak current dependence on SW amplitude was linear in range 5-60 mV
259 with the slope $89.52 \pm 0.14 \text{ AV}^{-1}$.
260 By of the CV reduction current dependence inspection of the Co(II)-Phen-PC
261 complex on the scan rate (v) in the range 1-100 mV/s, linear dependence of the
262 reduction current with the shift of the reduction potential towards negative values
263 confirmed that mechanism is irreversible with the reactant adsorption. Mixed ligand
264 complex reduction current increased exponentially with $v^{1/2}$.

265 Furthermore, reactant adsorption of the irreversible reduction process revealed that
266 the reduction peak width at half-height, satisfied the relationship $\Delta E_{p/2} \text{ (mV)} = (63.5 \pm$
267 $0.5)/\alpha n$, where $n = 2$ (number of simultaneously transferred electrons) and where α is
268 the average transfer coefficient [29,30]. From the experimental data calculated peak
269 width at half-height of Co(II)-Phen was $E_{p/2} = 73 \text{ mV}$ and relates to $\alpha = 0.5 \pm 0.05$,
270 while for Co(II)-Phen-PC complex was $E_{p/2} = 85 \text{ mV}$ and relates to $\alpha = 0.37 \pm 0.02$.

271 According to equation:

$$i_p = (5 \pm 1) \times 10^2 q a n^2 F a f \Delta E \Gamma \quad (1)$$

from the slope i_p/α using values $\alpha_{\text{Co(II)-Phen-PC}} = 0.37$, $n = 2$ and $q = 0.004 \text{ cm}^2$ (the surface of the mercury drop), $F = 96\,485 \text{ s A mol}^{-1}$ (Faraday constant) and $\Delta E = 20 \text{ mV}$ (square-wave scan increment) the amount of the adsorbed reactant (Γ) was calculated. Co(II)-Phen-PC complex maximum concentration adsorbed at the mercury drop electrode amount to $\Gamma = (1.45 \pm 0.12) \times 10^{-10} \text{ mol cm}^{-2}$.

Conditional stability constants and apparent stoichiometry of Co(II) complexes were determined by CLE/ACSV method [31]. The method was described as competitive ligand equilibrium (CLE) followed by adsorptive cathode stripping measurements (ACSV). The conditional stability constant for Co(II)-Phen was determined using Nitriolotriacetic acid (NTA) as a competitive ligand [16, 32], while for Co(II)-Phen-PC complex Phen. Conditional stability constant was calculated based on following equations.

$$c_{\text{Co}} = [\text{Co}'] + [(\text{CoPhen})_n] + [(\text{CoNTA})] \quad (2)$$

or for the mixed complex:

$$c_{\text{Co}} = [\text{Co}'] + [(\text{CoPhen}_x\text{PC}_y)_n] + [(\text{CoPhen})_n]^* \quad (3)$$

where $[\text{Co}']$ is the sum of concentrations of all inorganic species $(\text{Co}(\text{OH})^+)$ and $\text{Co}(\text{OH})_2$ and $\text{Co}(\text{Phen})_n$, $\text{Co}(\text{Phen}_x\text{PC}_y)_n$ (complex of Co with n molecules of ligand). $[(\text{CoNTA})_n]$ represents the concentration quantity of all present Co(II) species with NTA or Phen* as a competitive ligand at given pH. Peak currents were directly related to $[(\text{CoPhen})_n]$ or $[(\text{CoPhen}_x\text{PC}_y)_n]$ through the proportionally factor S:

$$I_p = S [(\text{CoPhen})_n] \quad (4)$$

$$I_p = S [(\text{CoPhen}_x\text{PC}_y)_n] \quad (5)$$

295 The ratio, X , of cobalt peak current in presence of 1,10-Phenanthroline as a
 296 competitive ligand ($i_{p,i}$) to one without it, $i_{p,0}$ can be written as

$$297 \quad X = i_p/i_{p,0} = [(\text{CoPhen})_n] / [(\text{CoPhen})_n] + [\text{CoNTA}] \quad (6)$$

$$298 \quad X = i_p/i_{p,0} = [(\text{CoPhen}_x\text{PC}_y)_n] / [(\text{CoPhen}_x\text{PC}_y)_n] + [(\text{CoPhen})_n]^* \quad (7)$$

299 Using expressions for $[(\text{CoPhen})_n]$ and $[(\text{CoPhen}_x\text{PC}_y)_n]$

$$300 \quad X = K_{\text{CoPhen}}^{\text{cond}}[\text{Phen}]_n / K_{\text{CoPhen}_2}^{\text{cond}}[\text{Phen}]_n + K_{\text{CoOHNTA}}[\text{NTA}]_n \quad (8)$$

$$301 \quad X = K_{\text{CoPhen}_x\text{PC}_y}^{\text{cond}}[\text{CoPhen}_x\text{PC}_y]_n / K_{\text{CoPhen}_x\text{PC}_y}^{\text{cond}}[\text{CoPhen}_x\text{PC}_y]_n + K_{\text{CoOHPhen}}[\text{Phen}]_n^* \quad (9)$$

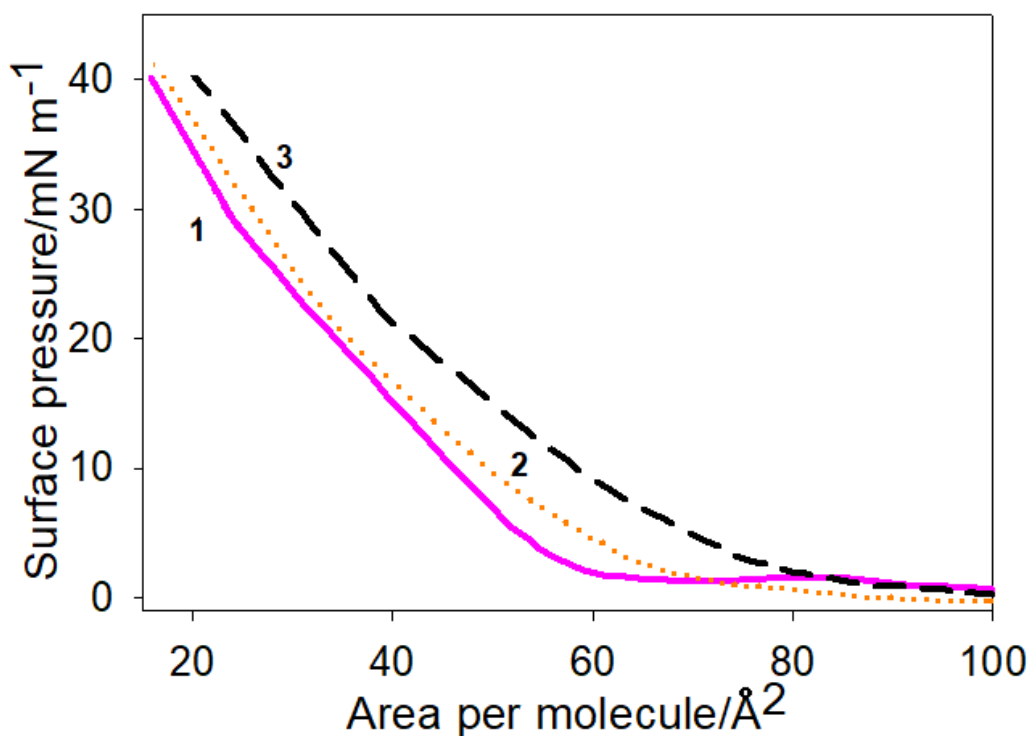
302 From the mean value of the experimentally obtained values it was calculated log
 303 $K_{\text{Co(II)-1,10-Phen}_2}$ to amount to 22.75 ± 0.48 . Obtained conditional constants amount to
 304 $\log K_{\text{Co(II)Phen}_2\text{PC}} = 23.02 \pm 0.26$ and $\log K_{\text{Co(II)Phen}_2\text{PC}_2} = 29.31 \pm 0.17$. The
 305 stoichiometry was determined so that the calculated curve agreed well with our
 306 experimental data (Fig. S2 A, B, C).

307

308 **3.2. Monolayer surface pressure - area measurements**

309 Monolayer studies at the air-water interface were performed to complement the
 310 voltammetric conclusions of the mixed ligand complex Co(II)-Phen-PC formation at a
 311 model hydrophobic interface. An aqueous solution of 0.55 mol dm^{-3} NaCl (pH = 8.2; 1
 312 mol dm^{-3} borate buffer) was used as pure subphase, while pure subphase with
 313 additions of Co(II) ions ($1 \times 10^{-5} \text{ mol dm}^{-3}$), Phen ($1.2 \times 10^{-5} \text{ mol dm}^{-3}$), and/or both
 314 Co (II) ions and Phen was further used for penetration experiments. The compression
 315 behavior of the PC monolayer on the pure subphase was firstly evaluated (Fig. 4,
 316 curve 1). At A_{max} ($> 60 \text{ \AA}^2$), PC molecules were in the liquid-expanded state with
 317 some degree of cooperative interaction but still not closely packed, as previously well
 318 described [33-36]. As the area per molecule decreased during the compression of the

319 monolayer, the surface pressure steadily increased due to the coexistence of liquid
 320 expanded and liquid condensed phases, reaching the maximal surface pressure.
 321 Determined A_{lim} of PC monolayer on pure subphase was 58 \AA^2 , which is in the range
 322 of the previous results. Penetration experiments were further performed during 3h at
 323 the constant A_{max} where PC monolayer was in the liquid-expanded phase, facilitating
 324 the interactions of the different subphase constituents with supporting monolayer. A
 325 comparison of the specific π - A isotherms of PC monolayer on pure subphase as a
 326 reference with those where additions of Co(II) ions ($1 \times 10^{-5} \text{ mol dm}^{-3}$) and both Co(II)
 327 ions and Phen, are present in subphase (Fig.5), enables information on the
 328 intermolecular interactions within the reference monolayer.



329 Fig 5. Surface pressure (π) - area (A) compression isotherms of the PC monolayer on
 330 a pure subphase ($0.55 \text{ mol dm}^{-3} \text{ NaCl}$; $1 \text{ mmol dm}^{-3} \text{ borate buffer}$) (1); pure
 331 subphase containing $c_{\text{Co}} = 1 \times 10^{-5} \text{ mol dm}^{-3}$ (2); $1 \times 10^{-5} \text{ mol dm}^{-3} \text{ Co(II)}$ + $1.2 \times$
 332 $10^{-5} \text{ mol dm}^{-3} \text{ Phen}$ (3); $\text{pH}=8.2$; $T = 294 \text{ K}$.

334 The π -A isotherms of the PC monolayer on a subphase containing Co(II) ions (Fig.
335 5, curve 2) showed that a weak interaction take place between the PC molecules
336 and the Co(II), allowing the PC molecules to pack more densely, i.e. to occupy a
337 smaller surface area, $A_{lim} = (53.0 \pm 0.5) \text{ \AA}^2$, relative to PC monolayer on pure
338 subphase (Fig.5, curve 1). The observed condensation effect is noticed for the
339 dipalmitoylphosphatidylcholine (DPPC) monolayers affected by the increasing
340 concentrations of Zn^{2+} in the subphase where dehydration of phosphate groups of
341 the DPPC occurred through direct interaction with metal ions [37]. The
342 neutralization processes within the lipid head-group moiety may change the local
343 conformation and have a general electrical screening effect [38-41]. The strength of
344 the interaction between the divalent ion and the lipid monolayer most likely increase
345 in the area of the lipid head-group, where the dielectric permittivity of the
346 environment and, thus, the electrostatic screening of the charges was reduced.

347 Compared to PC monolayer on a subphase containing Co(II) ions, an increase of
348 A_{lim} to $(64.0 \pm 0.8) \text{ \AA}^2$ was observed when of Co(II) and Phen were present in the
349 subphase (Fig. 5, curve 3). Both components present in the subphase, thus,
350 affected the surface organization of the PC monolayer, resulting in a more
351 expanded film. The observed expansion effect was different from the previously
352 detected condensation effect due to the presence of Co (II) ions (without Phen) in
353 the subphase. Since Phen was not absorbed on the PC monolayer itself (isotherm
354 identical to PC on pure subphase, not shown), we hypothesized that the observed
355 effect of expansion on the incorporation of Co (II) -Phen complex into the PC
356 monolayer and the formation of Co (II) -Phen-PC complex is the explanation for
357 such behavior.—This is supported by the fact that the expansion of PC in the
358 subphase Co (II) + Phen in relation to the reference PC monolayer occurred even

359 at the highest surface pressures. This indicates the strong incorporation of
 360 dissolved forms into the carrier monolayer of PC molecules, so that, “extrusion”
 361 from the lipid head region was not observed in the tightly packed state of the
 362 monolayer [34,37].

363 The expansion of the π -A isotherms, as a result of the interaction between the lipid
 364 monolayer and solutes from the subphase, was commonly interpreted as
 365 penetration or incorporation of the solute forms into the supporting monolayer
 366 [42,43]. It is worth noting that the isotherms of the subphase containing only Co(II)
 367 ions or Phen in the absence of the PC layer at the surface did not show significant
 368 adsorption at the interface itself (data not shown), as reported previously [44]. The
 369 observed effects with the monolayer study supported previous electrochemical
 370 findings on the Co(II) -Phen complex binding within the PC layer and formation of a
 371 mixed Co(II)-Phen-PC complex at the surface.

372 The equilibria of observed system at the air-water interface can be described by
 373 following chemical reactions:



376 and the equilibrium state of the system could be described by following equations:

$$377 \quad K1 = \frac{c_{\text{PCCo}^{2+}}}{c_{\text{PC}} * c_{\text{Co}^{2+}}} \quad (12)$$

$$378 \quad K2 = \frac{c_{\text{PCCo}^{2+}\text{Phen}_2}}{c_{\text{PCCo}^{2+}} * c^2_{\text{Phen}}} \quad (13)$$

$$379 \quad c_{\text{PC}} * A_{\text{PC}} + c_{\text{PCCo}^{2+}} * A_{\text{PCCo}^{2+}} + c_{\text{PCCo}^{2+}\text{Phen}_2} * A_{\text{PCCo}^{2+}\text{Phen}_2} = 1 \quad (14)$$

$$380 \quad c_{\text{PC}} + c_{\text{PCCo}^{2+}} + 2c_{\text{PCCo}^{2+}\text{Phen}_2} = C \quad (15)$$

381 where C_{PC} , $C_{PCCo^{2+}}$, $C_{PCCo^{2+}Phen_2}$ (mol m^{-2}) are the surface concentrations of
 382 components PC, $PCCo^{2+}$, $PCCo^{2+}Phen_2$; $C_{Co^{2+}}$ (mol m^{-3}) is the concentration of Co^{2+}
 383 ions; A_{PC} , $A_{PCCo^{2+}}$, $A_{PCCo^{2+}Phen_2}$ ($\text{m}^2 \text{mol}^{-1}$) are surface areas occupied by 1 mol of
 384 components PC, $PCCo^{2+}$, $PCCo^{2+}Phen_2$. K_1 ($\text{m}^3 \text{mol}^{-1}$) K_2 ($\text{m}^2 \text{mol}^{-1}$) are the stability
 385 constants of systems $PCCo^{2+}$ and $PCCo^{2+}Phen_2$, and C (mol m^{-2}) is the total surface
 386 concentration.

387 Multiple linear regression was performed, following the established procedure
 388 described in details previously [45,46], K_1 , K_2 , A_{PC} , $A_{PCCo^{2+}}$, $A_{PCCo^{2+}Phen_2}$ were
 389 calculated. Equations used are shown following instructions from the literature [34]:

$$390 \quad A_{PC} = (-m_3)/b \quad (16)$$

$$391 \quad A_{PCCo} = (-m_1)/m_4 \quad (17)$$

$$392 \quad A_{PCCoPhen} = 2(A_{PC} * m_4 - A_{PCCo} * b)/(m_4 - b) \quad (18)$$

$$393 \quad K_1 = -\frac{2 * A_{PCCo^{2+}} - A_{PCCo^{2+}Phen_2}}{m_4 * K_2 * A^2 PCCo^{2+} Phen_2} \quad (19)$$

$$394 \quad K_2 = -\frac{(2A_{PC} - A_{PCCo^{2+}Phen_2}) + (2A_{PCCo^{2+}} - A_{PCCo^{2+}Phen_2})}{4 + m_5 * A^2 PCCo^{2+} Phen_2} \quad (20)$$

395 The stability constant of the PC-Co system (1:1) was calculated to amount to $K_1 = 2.4$
 396 $\times 10^{-2} \text{ m}^3 \text{mol}^{-1}$, while $K_2 = 4.86 \times 10^{10} \text{ m}^2 \text{mol}^{-1}$ upon the addition of Phen describing
 397 Pc-Co-Phen₂ system the air-water boundary. Although the monolayer study at the
 398 air-water interface was accomplished to complement the electrochemical results, it is
 399 important to note that the obtained complex constants calculated based on the
 400 electrochemical and monolayer data, are not comparable due to the different
 401 approaches applied. Although a single-layer air-water boundary study was conducted
 402 to confirm the electrochemical results, it is important to note that the equilibrium
 403 constants obtained based on electrochemical and monolayer data, are not
 404 comparable due to the application of different approaches. However, both constant

405 types showed higher stability of the mixed complex than the stability of the Co(II)-
406 Phen or Co(II)-Phen-PC complex.

407

408 Conclusion

409 The penetration of cobalt (II) as one of the crucial micronutrient in numerous
410 biological processes, through the cell membrane is important for understanding its
411 fate and role in the marine environment living organisms. Studies of PC adsorbed on
412 hydrophobic surfaces (mercury drop electrode and air-water interface) used as a
413 model for a cell membrane, showed that direct binding between Co(II) and PC is very
414 weak, and not registered by electrochemical measurements. Conditional Stability
415 Constants of the complexes are essential for assessing the ability of ligands to bind
416 micronutrients under actual conditions. The study of the ligand substitution
417 mechanism in the Co(II) coordination sphere enable to predict the micronutrients
418 behavior in biological processes. Co(II) complexation takes place with Phen forming
419 a stable complex with a stoichiometry of 1:2. Co (II)-Phen complex with conditional
420 stability constant $\log K_{\text{Co(II)-1,10-Phen}_2} = 22.75 \pm 0.48$. Co (II)-Phen complex as an
421 intermediate interacts with PC molecules by substituting two remained water
422 molecules in its coordination sphere resulting most probably in the stable octahedral
423 configuration. In that way is formed hydrophobic mixed ligand complex Co(II)-Phen-
424 PC. The mixed ligand complex reduction occurs at about -1.5 V by an irreversible
425 mechanism, followed by dissociation, leaving only PC molecules adsorbed at the
426 electrode surface (EC mechanism). The net stoichiometry of the mixed ligand
427 complexes formed at the mercury drop electrode was calculated to be 1:2:1 and 1:2:2
428 for Co:Phen:PC. The conditional stability constants of mixed ligand complexes were
429 calculated to amount $\log K_{\text{Co(II)Phen}_2\text{PC}} = 23.02 \pm 0.26$ and $\log K_{\text{Co(II)Phen}_2\text{PC}_2} = 29.31 \pm$

430 0.17 ($I_c = 0.55$). The quantity of adsorbed reactant (Γ) Co (II)-Phen-PC complex was
431 *calculated to be* $(1.45 \pm 0.12) \times 10^{-10}$ mol cm⁻². The totally irreversible mechanism of
432 reduction with adsorption of the reactant was confirmed by examining the reduction
433 current and potential in dependence on the SW frequency and amplitude, as well as
434 by examining the SW forward and backward current. Our electrochemical
435 measurement results were supported by experiments at the air-water interface. The
436 change in the parameters of obtained π -A isotherms indicated a penetration of Co(II)-
437 Phen complex into the supporting PC monolayer. A weak stability constant of the PC-
438 Co system (1:1) at the air-water interface was determined to be $K_1 = 2.4 \times 10^{-2}$ m³
439 mol⁻¹. Obtained PC isotherms affected by the addition of both Co(II) ions and Phen in
440 the subphase, indicated a possibility of a mixed ligand complex formation.
441 Furthermore, calculated stability constant for described system amount to $K_2 = 4.86 \times$
442 10^{10} m² mol⁻¹. This study, performed at model hydrophobic surfaces, is a base for a
443 better understanding of the cobalt (II) - lipid association mechanism in
444 biogeochemical processes mediated by cell membranes, with particular relevance to
445 the marine environment.

446

447 Acknowledgement

448 The financial support for this work was provided by BiREADI project IP-2018-01-3105
449 (Biochemical responses of oligotrophic Adriatic surface ecosystems to atmospheric
450 deposition inputs), funded by the Croatian Science Foundation.

451

452 References:

453

454 [1] K. W. Bruland, J. R. Donat, D. A. Hutchins, Interactive influences of bioactive
455 trace metals on biological production in oceanic waters, *Limnol. Oceanogr.*, 36(8)
456 (1991) 1555; doi:[10.4319/LO.1991.36.8.1555](https://doi.org/10.4319/LO.1991.36.8.1555)

457

458 [2] E. I. Hamilton, The geobiochemistry of cobalt, *Sci. Total Environ.*, 150 (1–3)
459 (1994) 7.; doi: [10.1016/0048-9697\(94\)90126-0](https://doi.org/10.1016/0048-9697(94)90126-0)

460

461 [3] K. N. Buck, M. C. Lohan, S. G. Sander, C. Hassler, and I. Pižeta, Editorial:
462 Organic ligands-A key control on trace metal biogeochemistry in the ocean, *Front.*
463 *Mar. Sci.*, 4 (2017) 1; doi: [org/10.3389/fmars.2017.00313](https://doi.org/org/10.3389/fmars.2017.00313)

464

465 [4] T. W. Lane, M. A. Saito, G. N. George, I. J. Pickering, R. C. Prince, F. M. M.
466 Morel, A cadmium enzyme from a marine diatom, *Nature*, 435 (2005),42;
467 doi: [10.1038/435042a](https://doi.org/10.1038/435042a)

468

469 [5] M. J. Ellwood, C. M. G. Van den Berg, Determination of organic complexation of
470 cobalt in seawater by cathodic stripping voltammetry, *Mar. Chem.*, 75(1-2) (2001) 33;
471 doi: [org/10.1016/S0304-4203\(01\)00024-X](https://doi.org/org/10.1016/S0304-4203(01)00024-X)

472

473 [6] M. A. Saito, J. W. Moffett, Complexation of cobalt by natural organic ligands in the
474 Sargasso sea as determined by a new high-sensitivity electrochemical cobalt
475 speciation method suitable for open ocean work, *Mar. Chem.*, 75 (1–2) (2001) 49;
476 doi: [org/10.1016/S0304-4203\(01\)00025-1](https://doi.org/org/10.1016/S0304-4203(01)00025-1)

477 [7] J. M. Vraspir, A. Butler, Chemistry of marine ligands and siderophores, Ann. Rev.
478 Mar. Sci., 1 (2009) 43; doi:[10.1146/annurev.marine.010908.163712](https://doi.org/10.1146/annurev.marine.010908.163712)

479

480 [8] Deenah Osman, Anastasia Cooke, Tessa R. Young, EvelyneDeery, Nigel J.
481 Robinson, Martin J. Warren, The requirement for cobalt in vitamin B12: A paradigm
482 for protein metalation, BBA - Molecular Cell Research 1868 (2021) 118896; doi:
483 [org/10.1016/j.bbamcr.2020.118896](https://doi.org/10.1016/j.bbamcr.2020.118896)

484

485 [9] Q. Z. Zhu, Robert Curwood Aller, Robert Curwood Aller, Aleya Kaushik, Analysis
486 of vitamin B12 in seawater and marine sediment porewater using ELISA, 2011
487 Limnology and Oceanography, Methods 9(10):515-523; doi:
488 [org/10.4319/lom.2011.9.515](https://doi.org/10.4319/lom.2011.9.515)

489

490 [10] A. Bencini and V. Lippolis, 1,10-Phenanthroline: A versatile building block for the
491 construction of ligands for various purposes, Coord. Chem. Rev., 254(17–18) (2010)
492 2096; doi: [org/10.1016/j.ccr.2010.04.008](https://doi.org/10.1016/j.ccr.2010.04.008)

493

494 [11] N. Fujisawa, K. Furubayashi, M. Fukushima, M. Yamamoto, T. Komai, K.
495 Ootsuka, Y. Kawabe, Evaluation of the Iron(II)-binding Abilities of Humic Acids by
496 Complexometric Titration using Colorimetry with ortho-Phenanthroline, Humic Sub
497 Res., 8 (2011) 1.

498

499 [12] R. Pichot, R. L. Watson, I. T. Norton, Phospholipids at the interface: Current
500 trends and challenges, Int. J. Mol. Sci., 14(6) (2013) 11767; doi:
501 [10.3390/ijms140611767](https://doi.org/10.3390/ijms140611767); doi: [10.3389/fimmu.2017.01513](https://doi.org/10.3389/fimmu.2017.01513)

502 [13] Y. Ma, K. Poole, J. Goyette, K. Gaus, Introducing membrane charge and
503 membrane potential to T cell signaling, *Front. Immunol.*, 8 (2017) 1; doi:
504 [10.3389/fimmu.2017.01513](https://doi.org/10.3389/fimmu.2017.01513)

505

506 [14] L. O. Gerlach, J. S. Jakobsen, K. P. Jensen, M. R. Rosenkilde, R. T. Skerlj, U.
507 Ryde, G. J. Bridge, T. W. Schwartz, Metal ion enhanced binding of AMD3100 to
508 Asp262 in the CXCR4 receptor, *Biochemistry*, 42(3) (2003), 710; doi:
509 [10.1021/bi0264770](https://doi.org/10.1021/bi0264770)

510

511 [15] J. J. Giner-Casares, G. Brezesinski, H. Möhwald, Langmuir monolayers as
512 unique physical models, *Curr. Opin. Colloid Interface Sci.*, 19(3) (2014) 176; doi:
513 [org/10.1016/j.cocis.2013.07.006](https://doi.org/10.1016/j.cocis.2013.07.006)

514

515 [16] A. Bačinić, L. M. Tumir, and M. Mlakar, Electrochemical characterization of
516 Cobalt(II)-Complexes involved in marine biogeochemical processes. I. Co(II)-4-
517 nitrocatechol and Co(II)-Humate, *Electrochim. Acta*, 337 (2020) 135797; doi:
518 [org/10.1016/j.electacta.2020.135797](https://doi.org/10.1016/j.electacta.2020.135797)

519

520 [17] S. M. Baumler, G. J. Blanchard, The Influence of Metal Ions on the Dynamics of
521 Supported Phospholipid Langmuir Films, *Langmuir*, 33(12) (2017) 2986; doi:
522 [org/10.1021/acs.langmuir.7b00042](https://doi.org/10.1021/acs.langmuir.7b00042)

523

524 [18] A. P. Serro, R. Galante, A. Kozica, P. Paradiso, A. M. P. S Gonçalves da Silva,
525 K. V. Luzyanin, A. C. Fernandes, B. Saramago, Effect of tetracaine on DMPC and

526 DMPC + cholesterol biomembrane models: Liposomes and monolayers, Colloids
527 Surfaces B Biointerfaces, 116 (2014) 63; doi: [10.1016/j.colsurfb.2013.12.042](https://doi.org/10.1016/j.colsurfb.2013.12.042)

528

529 [19] V. P. N. Geraldo, F. J. Pavinatto, T. M. Nobre, L. Caseli, O. N. Oliveira, Langmuir
530 films containing ibuprofen and phospholipids, Chem. Phys. Lett., 559 (2013), 99; doi:
531 [10.1016/j.cplett.2012.12.064](https://doi.org/10.1016/j.cplett.2012.12.064)

532

533 [20] J. J. Leitch, C. L. Brosseau, S. G. Roscoe, K. Bessonov, J. R. Dutcher, J.
534 Lipkowski, Electrochemical and PM-IRRAS characterization of cholera toxin binding
535 at a model biological membrane, Langmuir, 29(3) (2013) 965; doi:
536 [org/10.1021/la304939k](https://doi.org/10.1021/la304939k)

537

538 [21] A. Akbarzadeh, R. Rezaei-sadabady, S. Davaran, S. W. Joo, N. Zarghami,
539 Liposome : classification , prepNew aspects of liposomesaration , and applications,
540 Nanoscale Res. Lett., 8(102) (2003) 1; doi: [org/10.1186/1556-276X-8-102](https://doi.org/10.1186/1556-276X-8-102)

541

542 [22] M. N. Jones, The surface properties of phospholipid liposome systems and their
543 characterisation, Adv. Colloid Interface Sci., 54 (1995) 93; doi: [10.1016/0001-](https://doi.org/10.1016/0001-8686(94)00223-y)
544 [8686\(94\)00223-y](https://doi.org/10.1016/0001-8686(94)00223-y)

545

546 [23] A. Nelson, N. Auffret, J. Borlakoglu, Interaction of hydrophobic organic
547 compounds with mercury adsorbed dioleoylphosphatidylcholine monolayers, BBA -
548 Biomembr., 1021(2) (1990) 205; doi: [org/10.1016/0005-2736\(90\)90035-M](https://doi.org/10.1016/0005-2736(90)90035-M)

549

550 [24] L. M. Pfeffer, B. C. P. Kwok B.C.P., F.R. Landsberger., I. Tamm, Interferon
551 stimulates cholesterol and phosphatidylcholine synthesis but inhibits cholesterol ester
552 synthesis in HeLa-S3 cells (human (3-interferon/lipid metabolism/membrane
553 structure/endocytosis/low density lipoprotein). Proc. Nati. Acad. Sci. USA 82 (1985)
554 2417–2421; doi:[10.1073/pnas.82.8.2417](https://doi.org/10.1073/pnas.82.8.2417)

555

556 [25] I. Čuljak, M. Mlakar, M. Branica, Synergetic adsorption of the copper-
557 phenanthroline-tributylphosphate complex at a mercury drop electrode, Anal. Chim.
558 Acta, 297(3) (1994) 427; doi: [org/10.1016/0003-2670\(94\)00225-8](https://doi.org/10.1016/0003-2670(94)00225-8)

559

560 [26] X. Liang, D. J. Campopiano, P. J. Sadler, Metals in membranes, Chem. Soc.
561 Rev., 36, (6) (2007) 968; doi: [org/10.1039/B617040B](https://doi.org/10.1039/B617040B)

562

563 [27] M. Zelić, Reverse Scan as a Source of Information in Square Wave
564 Voltammetry, Croat. Chem. Acta 79 (1) (2006) 49

565

566 [28] M. Lovrić and Š. Komorsky-Lovrić, Theory of Square-Wave Voltammetry of Two-
567 Electron Reduction with the Adsorption of Intermediate, International Journal of
568 Electrochemistry, 2012, (2012) 7; doi: [org/10.1155/2012/596268](https://doi.org/10.1155/2012/596268)

569

570 [29] M. Lovrić, Š. Komorsky-Lovrić, R. W. Murray, Adsorption effects in square-wave
571 voltammetry of totally irreversible redox reactions, Electrochim. Acta, 33(6) (1988)
572 739; doi: [org/10.1016/S0013-4686\(98\)80002-9](https://doi.org/10.1016/S0013-4686(98)80002-9)

573

574 [30] E. L. Rue, K. W. Bruland. Complexation of iron(III) by natural organic ligands in
575 the central North Pacific as determined by a new competitive ligand
576 equilibration/adsorptive cathodic stripping voltammetric method, Mar. Chem. 50
577 (1995) 117–138; doi.org/[10.1016/0304-4203\(95\)00031-L](https://doi.org/10.1016/0304-4203(95)00031-L)

578

579 [31] P. Vukosav, V. Tomišić, M. Mlakar, “Iron(III)-complexes engaged in the
580 biochemical processes in seawater. II. Voltammetry of Fe(III)-malate complexes in
581 model aqueous solution, Electroanalysis, 22(19) (2010) 2179; doi:
582 [org/10.1002/elan.200900632](https://doi.org/10.1002/elan.200900632)

583

584 [32] G. L. Gaines, Insoluble monolayers at liquid-gas interfaces, Academic press, New
585 York 1966, p. 254; doi: [10.1007/978-94-011-2272-6_3](https://doi.org/10.1007/978-94-011-2272-6_3)

586

587 [33] A. Aroti, E. Leontidis, M. Dubois, T. Zemb, G. Brezesinski, Monolayers, bilayers
588 and micelles of zwitterionic lipids as model systems for the study of specific anion
589 effects. Colloids Surf A. 303 (2007) 144–158., doi: [10.1016/j.colsurfa.2007.03.011](https://doi.org/10.1016/j.colsurfa.2007.03.011).

590

591 [34] M. Sovago, M. W. H. George, M. S. Wurpel, M. Müller, M. Bonn, Calcium-
592 induced phospholipid ordering depends on surface pressure. J Am Chem Soc. 129
593 (2007) 11079–11084. doi: [10.1021/ja071189i](https://doi.org/10.1021/ja071189i).

594

595 [35] A. D. Petelska, Z. A. Figaszewski, Phosphatidylcholine - Mg²⁺ equilibria in a
596 monolayer at the air/water interface. Open Chem. 11 (2013) 424–429; doi:
597 [10.2478/s11532-012-0170-7](https://doi.org/10.2478/s11532-012-0170-7)

598

599 [36] P. Laszuk, W. Urbaniak, A. D. Petelska, The Equilibria in Lipid–Lipoic Acid
600 Systems Monolayers, Microelectrophoretic and Interfacial Tension Studies,
601 Molecules, 25(16) (2020), 3678; doi:[org/10.3390/molecules25163678](https://doi.org/10.3390/molecules25163678)

602

603 [37] S. Li, L. Du, N. T. Tsona, W. Wang, The interaction of trace heavy metal with
604 lipid monolayer in the sea surface microlayer, Chemosphere 196 (2018) 323–330;
605 doi: [org/10.1016/j.chemosphere.2017.12.157](https://doi.org/10.1016/j.chemosphere.2017.12.157)

606

607 [38] M. Bara, A. Guiet-Bara, J. Durlach, Analysis of magnesium membraneous
608 effects:

609 612 binding and screening, Magnes Res 29 (1990) 4121–4128; [pmid: 3274925](https://pubmed.ncbi.nlm.nih.gov/3274925/)

610

611 [39] Adams, E.M., Casper, C.B., Allen, H.C., Effect of cation enrichment on
612 dipalmitoylphosphatidylcholine (DPPC) monolayers at the air-water interface, J.
613 Colloid Interface Sci. 478(2016) 353–364;doi: [10.1016/j.jcis.2016.06.016](https://doi.org/10.1016/j.jcis.2016.06.016)

614

615 [40] S. Kewalramani, H. Hlaing, B.M. Ocko, I. Kuzmenko, M. Fukuto Effects of
616 divalent cations on phase behavior and structure of a zwitterionic phospholipid
617 (DMPC) monolayer at the air–water interface. J Phys Chem Lett 1 (2010) 489–498,
618 doi: [org/10.1021/jz9002873](https://doi.org/10.1021/jz9002873)

619

620 [41] A. D. Petelska, M. Naumowicz, M. The effect of divalent ions on L- α -
621 phosphatidylcholine from egg yolk monolayers at the air/water interface, J Biol Inorg
622 Chem 22 (2017)1187–1195; doi: [org/10.1007/s00775-017-1495-7](https://doi.org/10.1007/s00775-017-1495-7)

623

624 [42] Z. Kozarac, B. Čosović, R. C. Ahuja, D. Moebius, W. Budach, Interaction of
625 Pyrene-3-sulfonate with Lipid Monolayers // Langmuir, 12(22) (1996) 5387-5392; doi:
626 [10.1021/la950908g](https://doi.org/10.1021/la950908g)

627

628 [43] Z. Kozarac, D. Möbius, D. B. Spohn, Investigation of Sea-surface Microlayer and
629 Phytoplankton Culture Samples by Monolayer Techniques and Brewster Angle
630 Microscopy, Croatica Chemica Acta, 71(2)(1998) 285-301

631

632 [44] R. Verger, F. Pattus, Lipid-Protein Interactions in Monolayers, Chemistry and
633 physics of lipids 30 (1982) 189-227; doi: [org/10.1016/0009-3084\(82\)90052-4](https://doi.org/10.1016/0009-3084(82)90052-4)

634

635 [45] M. Ivanova, M. G., Verger, R., Bois, A. G., Panaiotov, I. Proteins at the air/water
636 interface and their inhibitory effects on enzyme lipolysis. Colloids Surf. 54 (1991)
637 279–296; doi: [org/10.1016/0166-6622\(91\)80067-X](https://doi.org/10.1016/0166-6622(91)80067-X)

638

639 [46] M. Mlakar, V. Cuculić, S. Frka, B. Gašparović, Copper-phospholipid interaction at
640 cell membrane model hydrophobic surfaces, Bioelectrochemistry, 120 (2018) 10; doi:
641 [org/10.1016/j.bioelechem.2017.11.004](https://doi.org/10.1016/j.bioelechem.2017.11.004)

642

643